Biomedicine & Pharmacotherapy 175 (2024) 116730

Contents lists available at ScienceDirect

Biomedicine & Pharmacotherapy

journal homepage: www.elsevier.com/locate/biopha

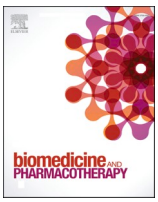

The AMPK activator ATX-304 alters cellular metabolism to protect against cisplatin-induced acute kidney injury

Marina Katerelos [a,b], Kurt Gleich [a,b], Geoff Harley [a,b], Kim Loh [c], Jonathan S. Oakhill [c], Bruce E. Kemp [c], David P. de Souza [d], Vinod K. Narayana [d], Melinda T. Coughlan [e,f], Adrienne Laskowski [e], Naomi X.Y. Ling [c], Lisa Murray-Segal [c], Robert Brink [g,h], Mardiana Lee [a,b], David A. Power [a,b,i], Peter F. Mount [a,b,i,*]

[a] Department of Nephrology, Austin Health, Heidelberg, Victoria 3084, Australia
[b] Kidney Laboratory, The Institute for Breathing and Sleep (IBAS), Austin Health, Heidelberg, Victoria 3084, Australia
[c] St. Vincent's Institute of Medical Research, Fitzroy, Victoria 3065, Australia
[d] Metabolomics Australia, Bio21 Institute of Molecular Science and Biotechnology, University of Melbourne, Parkville, Victoria 3052, Australia
[e] Glycation, Nutrition and Metabolism Laboratory, Department of Diabetes, Central Clinical School, Monash University, Melbourne, Victoria 3004, Australia
[f] Drug Discovery Biology, Monash Institute of Pharmaceutical Sciences, Monash University Parkville Campus, Parkville, Victoria 3052, Australia
[g] Immunology Division, Garvan Institute of Medical Research, Darlinghurst, New South Wales 2010, Australia
[h] St. Vincent's Clinical School, University of New South Wales, St. Vincent's Hospital, Darlinghurst, New South Wales 2010, Australia
[i] Department of Medicine (Austin), The University of Melbourne, Heidelberg ,Victoria 3084, Australia

ARTICLE INFO

Keywords:
AMP-activated protein kinase
Acute kidney injury
Cisplatin-induced AKI
Renal energy metabolism
ATX-304

ABSTRACT

Acute kidney injury (AKI) disrupts energy metabolism. Targeting metabolism through AMP-activated protein kinase (AMPK) may alleviate AKI. ATX-304, a pan-AMPK activator, was evaluated in C57Bl/6 mice and tubular epithelial cell (TEC) cultures. Mice received ATX-304 (1 mg/g) or control chow for 7 days before cisplatin-induced AKI (CI-AKI). Primary cultures of tubular epithelial cells (TECs) were pre-treated with ATX-304 (20 μM, 4 h) prior to exposure to cisplatin (20 μM, 23 h). ATX-304 increased acetyl-CoA carboxylase phosphorylation, indicating AMPK activation. It protected against CI-AKI measured by serum creatinine (control 0.05 ± 0.03 mM vs ATX-304 0.02 ± 0.01 mM, $P = 0.03$), western blot for neutrophil gelatinase-associated lipocalin (NGAL) (control 3.3 ± 1.8-fold vs ATX-304 1.2 ± 0.55-fold, $P = 0.002$), and histological injury (control 3.5 + 0.59 vs ATX-304 2.7 + 0.74, $P = 0.03$). In TECs, pre-treatment with ATX-304 protected against cisplatin-mediated injury, as measured by lactate dehydrogenase release, MTS cell viability, and cleaved caspase 3 expression. ATX-304 protection against cisplatin was lost in AMPK-null murine embryonic fibroblasts. Metabolomic analysis in TECs revealed that ATX-304 (20 μM, 4 h) altered 66/126 metabolites, including fatty acids, tricarboxylic acid cycle metabolites, and amino acids. Metabolic studies of live cells using the XFe96 Seahorse analyzer revealed that ATX-304 increased the basal TEC oxygen consumption rate by 38%, whereas maximal respiration was unchanged. Thus, ATX-304 protects against cisplatin-mediated kidney injury via AMPK-dependent metabolic reprogramming, revealing a promising therapeutic strategy for AKI.

1. Introduction

Acute kidney injury (AKI) is associated with severe morbidity and mortality, as well as a greater risk of chronic kidney disease [1,2]. The susceptibility of the kidney to injury relates to its energy requirements arising from its demand for adenosine triphosphate (ATP) to drive active transport [3]. Exposure to nephrotoxins such as chemotherapeutics and antibiotics is a common cause of AKI [4]. The cancer drug cisplatin is highly toxic to renal tubular cells, with cisplatin-induced AKI (CI-AKI) a common and dose limiting toxicity. In a cohort study, high-dose cisplatin for cancer caused severe AKI in 20%, impacting on long-term kidney function and patient survival [5]. The absence of targeted therapies to prevent and treat AKI has been identified as a contributor to poor patient outcomes and high mortality associated with AKI [6].

* Correspondence to: Department of Nephrology, Austin Health, Heidelberg, Victoria 3084, Australia.
E-mail address: Peter.Mount@austin.org.au (P.F. Mount).

https://doi.org/10.1016/j.biopha.2024.116730
Received 5 January 2024; Received in revised form 2 May 2024; Accepted 7 May 2024
Available online 14 May 2024

Dysregulation of energy metabolism is a common feature of AKI, with these pathways representing new potential therapeutic targets [3]. Renal tubular cells have an abundance of mitochondria, and mitochondrial dysfunction has been identified as a treatment target for renal tubular injury [3] Mitochondrial fatty acid β-oxidation (FAO) is the preferred source of ATP in the kidney, and its dysfunction results in ATP depletion and lipotoxicity, leading to tubular injury, inflammation, and development of renal fibrosis [7,8]. Improving energy metabolism and mitochondrial function is a promising strategy for AKI prevention and treatment [7].

AMP-activated protein kinase (AMPK) is a master regulator of metabolism with important roles in the kidney, including regulation of cellular energy balance, ion transport, cell growth, inflammation, and cell survival [9]. AMPK is activated by adenosine monophosphate (AMP) binding to the γ subunit, resulting in phosphorylation of the catalytic α subunit residue Thr^{172} [10]. Activation of AMPK maintains energy balance by activating catabolic processes such as fatty acid oxidation, glycolysis, and autophagy, while suppressing anabolic processes such as protein synthesis and lipid synthesis [11,12]. AMPK activation protects against various forms of AKI, including ischemia-reperfusion injury, sepsis, and AKI from nephrotoxins such as cisplatin [13–16].

ATX-304 is a pan-AMPK activator with mechanisms of action distinct from other AMPK activators [17,18]. Unlike indirect AMPK activators, such as metformin, ATX-304 has a direct effect on AMPK activity by preventing protein phosphatase 2C mediated dephosphorylation of p-$αThr^{172}$ [17]. In lung fibroblast cells, ATX-304 increased ATP levels [17]. Furthermore, the effects of ATX-304 differ from other direct activating pan-AMPK activators that act through the allosteric drug and metabolite (ADaM) binding site [18]. Direct AMPK activators, such as MK-8722, that bind to the ADaM site are associated with intracellular accumulation of glycogen [19], whereas this is not observed with ATX-304 [18]. This difference was recently attributed to ATX-304, also acting as a mitochondrial uncoupler, where mitochondrial electron transport is dissociated from ATP synthesis [18]. Thus, ATX-304 appears to function as a dual AMPK activator and mitochondrial uncoupler, contributing to its benefits in improving glucose levels and cardiac function [18]. In a phase 2a human trial, ATX-304 was well tolerated, lowered glucose and blood pressure, and improved microvascular perfusion [17]. ATX-304 activates AMPK in the kidney, where it protects against age-related fibrosis by promoting energy metabolism and autophagy [20]. Transcriptomic sequencing of the kidney revealed that ATX-304 induced fatty acid metabolism and mitochondrial biogenesis, while downregulating cellular aging and the DNA damage response [20]. These data suggest ATX-304 is a promising agent for kidney disease; however, its effects on tubular cell injury and AKI are unknown. This study aims to investigate whetherATX-304 treatment activates AMPK in the kidney to protect against cisplatin-induced injury.

2. Methods

2.1. Animal studies

All animal experiments were approved by the Austin Health Animal Ethics Committee (project number A2020_05679) and experiments are described according to the ARRIVE reporting guidelines [21]. Male C75Bl/6 mice were assigned to either chow containing ATX-304 (1 mg/g) (304-chow diet) or a control-chow diet for 7 days prior to establishing CI-AKI by intraperitoneal administration of cisplatin (20 mg/kg), administered as 2 × 10 mg/kg doses 4 h apart, in mice 11–14 weeks old [14] (n = 8 per group, 4 mice per cage, total mice used n = 48). The rationale for using male mice in the experiments was to reduce the risk of sex related variation in the AKI outcome. The 304-chow and control-chow diets were continued after the induction of CI-AKI, and the outcomes were studied after 2 days. Whole blood was collected by retro-orbital bleeding, and serum was sent to IDDEX laboratories (Victoria, Australia) for the measurement of creatinine levels. Both kidneys were removed for tissue analysis.

2.2. Primary kidney tubular epithelial cell cultures

Primary cultures of renal tubular epithelial cells (TECs) were prepared from female mice (aged 4–8 weeks) by sieving mouse kidney cortices through 100 μm cell strainers (Corning), as previously described [22]. Our rationale for using female mice for the TEC cultures is firstly to follow the principle of reduction in our experimental program, such that both male and female animals from the mouse breeding are utilized in experiments, and secondly to increase the sex generalizability of the experimental results.

2.3. Immortalized murine embryonic fibroblasts

AMPK-null and wild-type (WT) immortalized murine embryonic fibroblasts (iMEFs) were generated as previously described [23]. In brief, MEFs were extracted from WT or homozygous AMPK β1β2 null embryos (12–14 days post-coitum) generated by crossing homozygous β1 and β2 null mice. WT and AMPK β1/2 double knockout (β1/2-dKO) MEFs were immortalized by Fugene HD-mediated transfection with an SV40 large T-antigen expression construct [23].

2.4. LDH and MTS assays

For the lactate dehydrogenase (LDH) cell lysis assay, 100 μL of tetrazolium salt WST was added to the LDH assay buffer (ab65393; LDH-Cytotoxicity Assay Kit). The percentage lysis was calculated as ([sample-background/maximum lysis-background] × 100). The background and maximum lysis samples were analyzed in triplicate, and the test samples had n = 5 or n = 6.

Cellular metabolic activity was assessed using an MTS assay (MTS Assay Kit; ab197010; Abcam) The MTS reagent was added to the cells, mixed, and incubated at 37 °C for 2 h. Values were subtracted from the background (cell culture media alone), and MTS activity was compared to cells cultured in SF CHO K1 media.

The iMEFs were used as described above but were seeded at 2×10^5 cells/well.

2.5. AMPK α1 and α2 knock-in mice

Prkaa1^{T183A} and *Prkaa2*^{T172A} mice, containing whole body knock-in (KI) mutations for AMPK-α1KI (T183A) and AMPK-α2 (T172A), respectively, were produced by the Mouse Engineering Garvan/ABR (MEGA) Facility using CRISPR/Cas9 gene targeting in C57BL/6 J mouse embryos following established molecular and animal husbandry techniques [24](Supplementary Fig S1).

2.6. Western blot analysis

Lysates were prepared from TEC and mouse kidneys and western blotting (WB) was performed as previously described [25]. Quantification of WB was performed by densitometry using Image J software, with glyceraldehyde 3-phosphate dehydrogenase (GAPDH) as a loading control. Antibodies against acetyl-CoA carboxylase (3676 S), phospho-AMPKα (Thr172) (2535), AMPKα (5831), GAPDH (5174), and cleaved caspase 3 (9661) were purchased from Cell Signaling Technology. Phospho-ACC (S79) (ab68191) and neutrophil gelatinase associated lipocalin (NGAL) (ab216462) antibodies were from Abcam.

2.7. Real-time polymerase chain reaction (qRT-PCR)

Quantitative Real-Time PCR was performed using the PowerTrack SYBR Green Master Mix (Applied Biosystems) on a QuantStudio 3 Real-Time PCR System (Applied Biosystems). The delta-delta Ct method was

used to calculate relative expression, with GAPDH as the reference gene, as reported previously [14,22]. All PCR reactions were performed in triplicates, on 96-well plates, with data presented being the average of the triplicates. The primer sequences used in this study are listed in Supplementary Table S2. Data are expressed as fold change relative to controls.

2.8. Histology

Kidney samples were fixed in 10% neutral buffered formalin (Sigma-Aldrich) and embedded in paraffin. Sections of 4 μm thickness were used for periodic acid-Schiff (PAS) staining. To determine kidney injury, as defined by tubular necrosis, cellular casts, and tubular injury, a semi-quantitative scoring method was used as previously described [14]. Score 0 represents an injury area less than 10%, whereas score 1,2,3, or 4 represent injuries involving 10%–25%, 25%–50%, 50%–75%, or >75% of the field, respectively. The investigator performing the scoring (GH) was blinded to the assigned experimental group. At least 10 randomly chosen fields under a microscope (×400) were evaluated for each mouse, and the average score was calculated.

2.9. Polar metabolites analysis

Polar metabolites mass spectrometry analysis was performed on an Agilent 6545 B series quadrupole time-of-flight mass spectrometer (QTOF MS) as described previously [26]. Targeted data matrices were generated using EL-MAVEN (version 0.12.1-beta-2-g8277b82a) with metabolite identification (Metabolomics Standard Initiative (MSI) level 1) based on the retention time and molecular masses matching an authentic standard [27]. The cleaned data matrix was imported into Metaboanalyst 5.0 (metaboanalyst.ca) for statistical analyses. Data were log-transformed and median-normalized prior to performing principal component, heatmap, and volcano plot analyses. Data quality was further determined by observing PBQC clustering.

2.10. Cell metabolism assays

Respiration and glycolysis of TECs from female C57Bl/6 mice were measured using the XFe96 Seahorse analyzer (Agilent Technologies, Santa Clara, CA, USA). Prior to the metabolism studies, TECs were treated with ATX-304 (20 μM, 4 h) or DMSO control. Glycolytic and mitochondrial function were analyzed according to Seahorse XF Glycolysis Stress Test and Seahorse XF Mito Stress Test protocols (Agilent Technologies, Santa Clara, CA, USA).

2.11. Statistics

Statistical analyses were performed using Prism version 9.0 (GraphPad Software, San Diego, CA, USA). Data are presented as the mean ± SD. Multiple group means were compared using one-way or two-way ANOVA, followed by a post hoc test. Sample sizes were determined by the number needed to identify differences based on previous similar work [14,22]. The comparison of means between two groups was performed using an unpaired *t*-test. $P < 0.05$ were considered significant. Statistical analysis of TEC metabolite profiles was performed using Metaboanalyst 5.0.

2.12. Supplementary methods file

Additional detail regarding methods for primary kidney tubular epithelial cell cultures, LDH and MTS assays, generation of AMPK α1 and α2 knock-in mice, qRT-PCR, histology, polar metabolites analysis, and cell metabolism assays are provided in the Supplementary Methods File.

3. Results

3.1. Part 1: Mouse studies with ATX-304 treatment in the cisplatin-induced AKI model

First, we treated WT C57/Bl6 with 304-chow (1 mg/g) for 9 days in the absence of AKI and found that this treatment increased phosphorylation of the AMPK-specific phosphosite at ACC-Ser^{79} in whole kidney lysates, indicative of AMPK activation in the kidney (Figs. 1A, 1B). Next, to determine the effect of this AMPK activation by ATX-304 on AKI, mice were fed control-chow or 304-chow (1 mg/g) for 7 days, then treated with cisplatin (20 mg/kg) or saline, and followed for 2-days after AKI induction, while remaining on the study diets. Protection against AKI by ATX-304 treatment was evident by WB for the AKI marker NGAL (control-chow 3.3 ± 1.8-fold increase vs. 304-chow 1.2 ± 0.55-fold increase, $P = 0.002$) (Figs. 1C, 1D). In addition, ATX-304 protected against CI-AKI measured at 48 h by serum creatinine (control-chow 0.05 ± 0.03 mM vs 304-chow 0.02 ± 0.01 mM, $P = 0.0037$) (Fig. 1E). The severity of injury with CI-AKI was further evaluated by histological analysis of PAS-stained sections, revealing typical features of CI-AKI, including tubular necrosis, tubular dilatation, tubular vacuolation (white arrows), and cast formation (black arrow) (Fig. 1F). The injury score, determined through blinded assessment, found less severe injury after cisplatin with 304-chow compared to control (control-chow 3.5 ± 0.59 vs 304-chow 2.7 ± 0.74, $P = 0.03$) (Fig. 1G).

Analysis of AKI markers by RT-PCR found ATX-304 reduced the induction of NGAL observed with CI-AKI (control-chow 99.6 ± 22.8-fold vs. 304-chow 35.2 ± 5.9-fold, $P = 0.006$) (Fig. 2A), with a similar trend to improvement observed for kidney injury molecule-1 (KIM-1) (control-chow 247.8 ± 107.8-fold vs. 304-chow 174.8 ± 33.4-fold, $P = 0.07$) (Fig. 2B). The inflammatory cytokine and injury marker interleukin-6 (IL-6) increased with CI-AKI in control diet mice ($P = 0.02$) but did not increase with CI-AKI with ATX-304 treatment (Fig. 2C). IL-6 levels were lower in AKI with ATX-304, however, this difference was not statistically significant (control-chow 167.0 ± 224.9-fold vs. 304-chow 31.5 ± 18.2-fold, P = 0.06) (Fig. 2C). The chemokine monocyte chemoattractant protein-1 (MCP-1) increased less with ATX-304 treatment during CI-AKI than control diet (CI-AKI control-chow 18.7 ± 5.1-fold vs CI-AKI 304-chow 10.4 ± 1.3-fold, $P = 0.048$) (Fig. 2D). Regarding necroptosis, receptor-interacting protein kinase 1 increased with CI-AKI in the control diet (P=0.03) but was unchanged with CI-AKI and ATX-304 treatment (Fig. 2E). Receptor-interacting protein kinase 3 increased less with the ATX-304 chow diet during CI-AKI than with the control diet (CI-AKI control-chow 6.9 ± 2.4-fold vs. 304-chow 4.9 ± 1.3-fold, $P = 0.02$) (Fig. 2F).

To summarize, in the in vivo data from the mouse CI_AKI experiments, we observed evidence for protection from ATX-304 against AKI using different outcome measures including serum creatinine, NGAL protein expression, histological injury score, and RNA expression of NGAL and MCP-1. RNA expression for KIM-1 and IL-6 also trended in the direction of protection against AKI with ATX-304 treatment, however, those differences were not significant, which may relate to limitations arising from the sample size, and the intrinsic variability in PCR data with these measures.

3.2. Part 2: Cell culture studies of the effect of ATX-304 in primary TEC cultures

3.2.1. ATX-304 activates AMPK in kidney tubular epithelial cells to protect against cisplatin toxicity

The effect of ATX-304 on AMPK activity in TECs was assessed by stimulation with increasing concentrations of ATX-304 (5 μM, 10 μM, 20 μM) for 4 h (Fig. 3A). WB analysis demonstrated dose-dependent AMPK activation, with phosphorylation of AMPK-αThr^{172} increased 1.8-fold ($P < 0.01$) with 20 μM ATX-304 (Fig. 3B). A more pronounced dose response was seen with ACC- Ser^{79} phosphorylation, with 20 μM

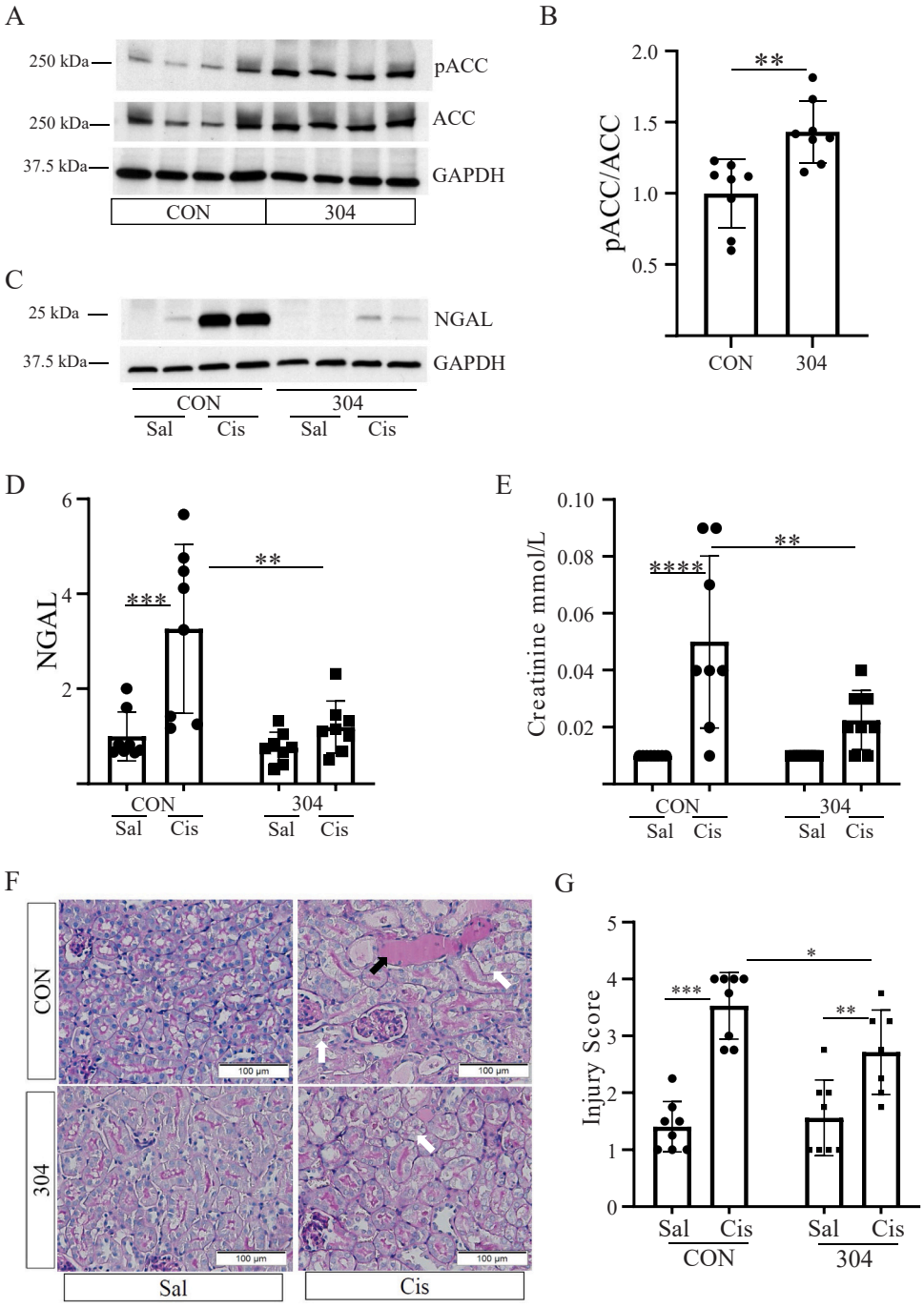

Fig. 1. ATX-304 protects against cisplatin-induced AKI. A. WB analysis of ACC phosphorylation in whole kidney lysates in mice treated with CON vs ATX-304 for 9 days (with IP Sal on D7). B. Densitometry analysis of ACC phosphorylation normalized to total ACC expression (n = 8). C and D. Wild type Male C57Bl/6 mice were fed control chow (CON) or chow containing ATX-304 (304) (1 mg/g) for 7 days, prior to injection with either cisplatin (Cis) or saline (Sal), with AKI outcomes analyzed at 48 h while remaining on the study diets (total time on diets of 9 days) (n = 8 per group). WB (1 C) and densitometry analysis (1D) for NGAL expression with Cis-AKI, comparing CON to ATX-304. E. Serum creatinine with Cis-AKI, comparing CON to ATX-304. F. Histological kidney injury was assessed by PAS-stain. Images were taken at 200× magnification. Scale bar of 100 µm is shown. Evidence of injury with cisplatin included cast formation (black arrow) and tubular injury with vacuolation and brush border loss (white arrows). G. Histological injury score. Uncropped western blots supporting the data in this figure are available in the supplementary material. *P <0.05 **P <0.01, ***P <0.001, ****P <0.0001.

ATX-304 causing a 6.4-fold increase (P < 0.0001) (Fig. 3C). Time-course analysis found ATX-304 (20 µM) activated AMPK within 1 h and that activation was still present after 4 h (Fig. 3D). The peak of activation was observed within 1 h as measured by both p-αThr^{172}-AMPK (4.5-fold increase, P < 0.01) and p-Ser^{79}-ACC (8.4-fold increase, P < 0.0001) (Fig. 3E-F). ATX-304 also activated AMPK in WT iMEFs (Fig. 3G).

The expression of selected genes that are important in energy metabolism after ATX-304 stimulation of TECs was studied by RT-PCR. Considering other studies indicating interactions between AMPK and other energy pathways such as sirtuins and the regulator of mitochondrial biogenesis, peroxisome proliferator-activated receptor-γ coactivator (PGC1α), we examined expression of molecules in these pathways [28]. Notably, expression of PGC1α was increased 3.5 ± 0.2-fold (Fig. 3H). The expression of acyl-CoA oxidase (ACox1), which is

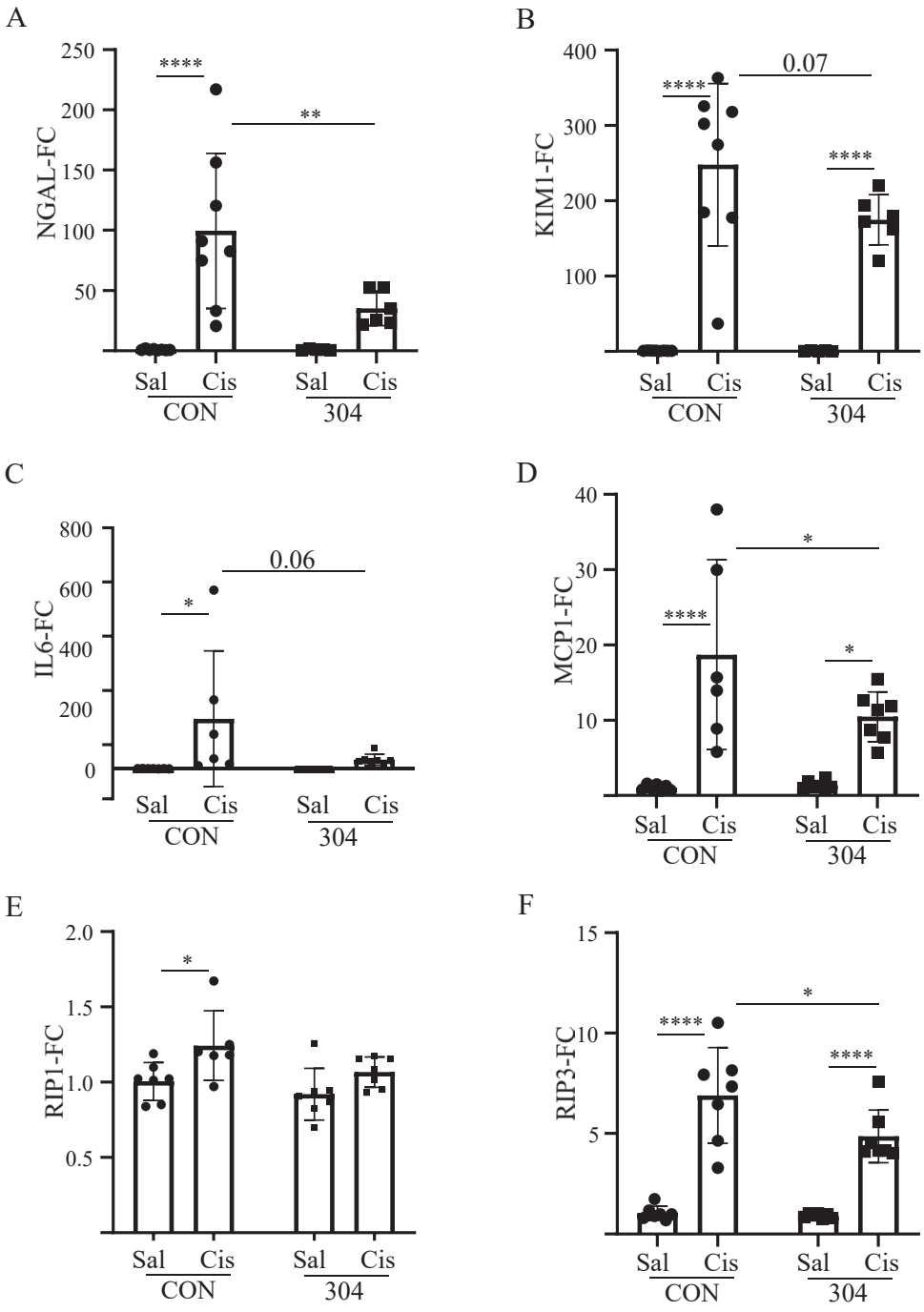

Fig. 2. Effect of ATX-304 on markers of CI-AKI severity measured by RT-PCR. Mice were fed control chow (CON) or ATX-304 chow (1 mg/g) for 7 days, prior to injection with cisplatin (Cis) or saline (Sal), with outcomes analyzed at 48 h (N = 8 animals per group, for each PCR reaction, RNA samples from 6 to 8 animals per group were randomly selected, within the limits of the number of samples that fit on a 96-well plate with samples and controls analyzed in triplicate). RT-PCR was performed for markers of injury (2 A NGAL, 2B KIM-1), inflammation (2 C IL-6, 2D MCP-1), and necroptosis (2E RIP1, 2 F RIP3). Y-axis unit are fold change (FC) compared to control and normalized for NGAL. *P <0.05, **P <0.01, ***P <0.001, ****P <0.0001).

important in peroxisomal fatty acid beta-oxidation, was unchanged (Fig. 3I). SIRT3, an important regulator of mitochondrial dynamics and fatty acid oxidation[30], was increased by 3.4 ± 0.2-fold (Fig. 3J). In contrast, SIRT1, which localizes to the nucleus[30], was reduced by 16 ± 0.2% (Fig. 3K).

To evaluate the effect of AMPK activation by ATX-304 on TEC injury, TECs were pre-treated with ATX-304 (20 μM, 4 h), ATX-304 was then removed from the culture media, prior to exposure to cisplatin (20 μM, 23 h). The effect of cisplatin on cell death was measured by LDH release, which showed that cisplatin caused cell lysis in TECs, which was prevented by pretreatment with ATX-304 (Fig. 4A). Cell viability was then analyzed by an MTS assay, showing cisplatin reduced TEC viability, which was rescued by ATX-304 pretreatment (Fig. 4B). To assess apoptosis, cleaved caspase 3 (CC3) WB analysis revealed that ATX-304 pre-treatment prevented the cisplatin-mediated increase in CC3 expression (Fig. 4C-D). In summary, analysis using different methods (LDH release, MTS assay, and WB for CC3) found pre-treatment with ATX-304 was highly effective in preventing cisplatin-mediated injury to TECs.

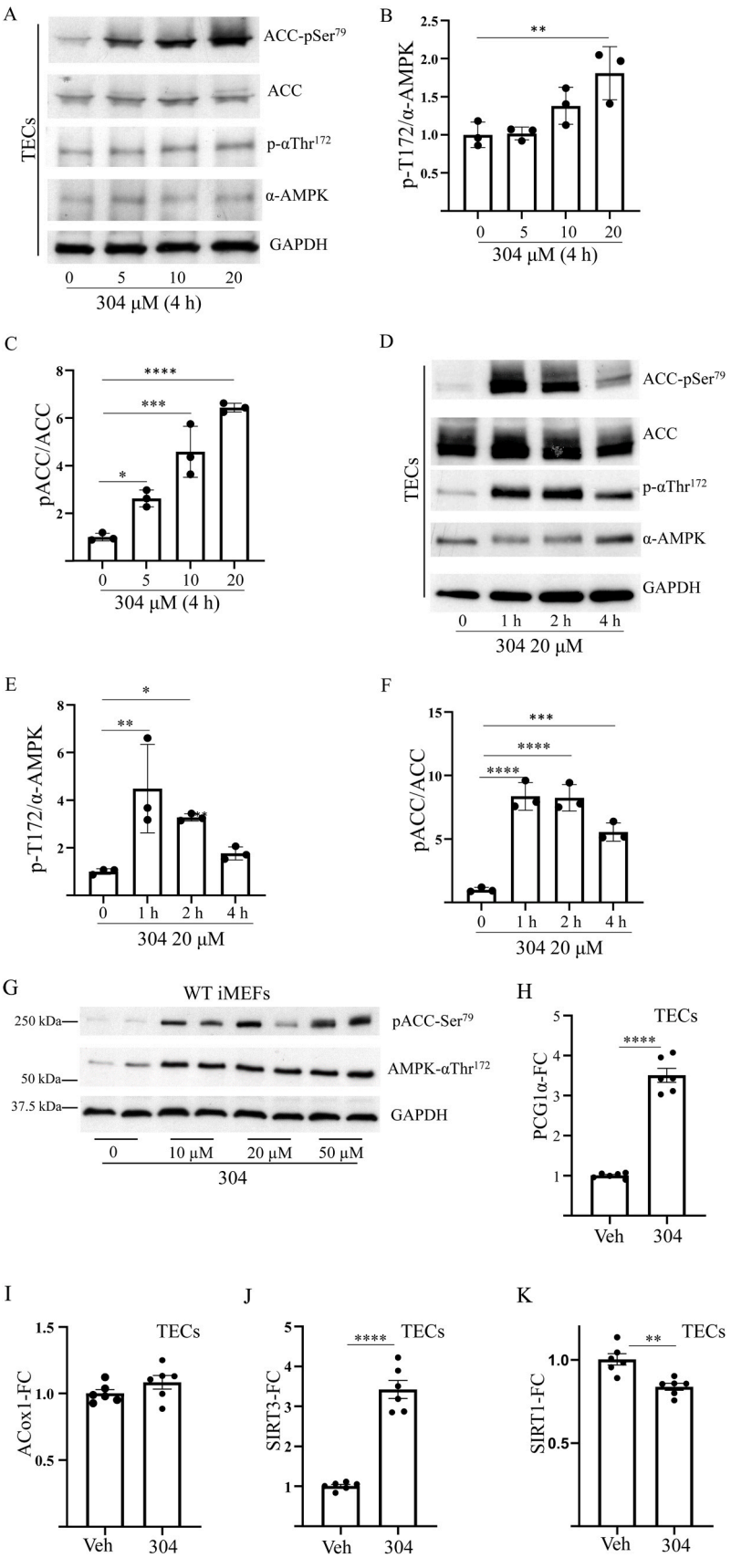

(caption on next page)

Fig. 3. Activation of AMPK in response to ATX-304 stimulation. 3 A. TECs were stimulated with increasing concentrations of ATX-304 (0 μM, 5 μM, 10 μM, 20 μM) for 4 h. Activated AMPK was analyzed by WB for phosphorylation at αThr^{172}, compared to total α1-AMPK, as well as its downstream substrate pACC-Ser^{79} and compared to total ACC. GAPDH is the loading control. Phosphorylation was quantified by densitometry for both p-αThr^{172}-AMPK (3B) and pACC-Ser^{79} (3 C). Data are mean ± s.d. of n = 3. One-way ANOVA, post hoc Dunnett's test (*P < 0.05, ** P < 0.01, ***P < 0.001, **** P < 0.0001). 3D. TECs were stimulated with ATX-304 (20 μM) for 1, 2 and 4 hours and lysates were analysed by western blot. Activation of αThr^{172}, compared to total α1-AMPK (3E), as well as pACC-Ser^{79} compared to total ACC (3 F), were quantified by densitometry. GAPDH is the loading control. Data are mean ± s.d. of n = 3. One-way ANOVA, post hoc Dunnett's test (*P < 0.05, ** P < 0.01, ***P < 0.001, **** P < 0.0001). 3 G. AMPK was also activated by ATX-304 (0 μM, 10 μM, 20 μM, 50 μM) for 4 h in mouse embryonic fibroblasts (iMEF). 3 H-3 K: Effect of ATX-304 stimulation (20 μM, 4 h) versus vehicle (Veh) on makers of energy metabolism in renal TECs was quantified by RT-PCR. PCG1α. ACox1, SIRT3, SIRT1 Y-axis units are fold change (FC) compared to Veh and normalized for GAPDH. *P < 0.05, ** P < 0.01, ***P < 0.001, **** P < 0.0001. Uncropped western blots supporting the data in this figure are available in the supplementary material.

3.2.2. *The role of AMPK in the protective effect of ATX-304 against cisplatin toxicity*

To determine whether the protective effect of ATX-304 was AMPK-dependent, we studied immortalized murine embryonic fibroblasts (iMEFs) null for AMPK (AMPK-β1/β2 KO iMEFs) [25]. The effect of ATX-304 on cell viability with cisplatin was studied in WT and AMPK-β1/β2 KO iMEFs. In preliminary experiments we found that MEFs were less sensitive to cisplatin toxicity than TECs, therefore a higher concentration of cisplatin was required in the MEF experiments than for TEC experiments. For MEFs, the effect of ATX-304 on cell viability was evaluated at two cisplatin concentrations (40 μM, 67 μM). ATX-304 increased cell viability in WT iMEFs; however, no protective effect of ATX-304 was observed in AMPK-β1/β2 KO iMEFs (Fig. 5A-B).

The catalytic AMPK α-subunit exists as two isoforms (α1 and α2), both of which are expressed in the kidney[31]. To determine the contribution of α1 and α2 heterotrimers to the protective effect of ATX-304 against cisplatin, TECs were isolated from AMPK α1 and α2 KI mice harboring Thr→Ala kinase activation loop mutations at Thr$^{172/183}$. The MTS assay found TECs from AMPK-α1KI mice were still afforded partial protection by ATX-304 against cisplatin, although this protection was reduced in AMPK-α1KI TECs compared to that in WT TECs (Fig. 5C). Similarly, TECs from AMPK-α2KI mice were also partially protected by ATX-304 against cisplatin, although protection was diminished in AMPK-α2KI TECs compared to WT TECs (Fig. 5D). To assess this further, we crossbred the AMPK-α1KI and AMPK-α2KI strains; however, this mating did not generate offspring homozygous for both α1 and α2

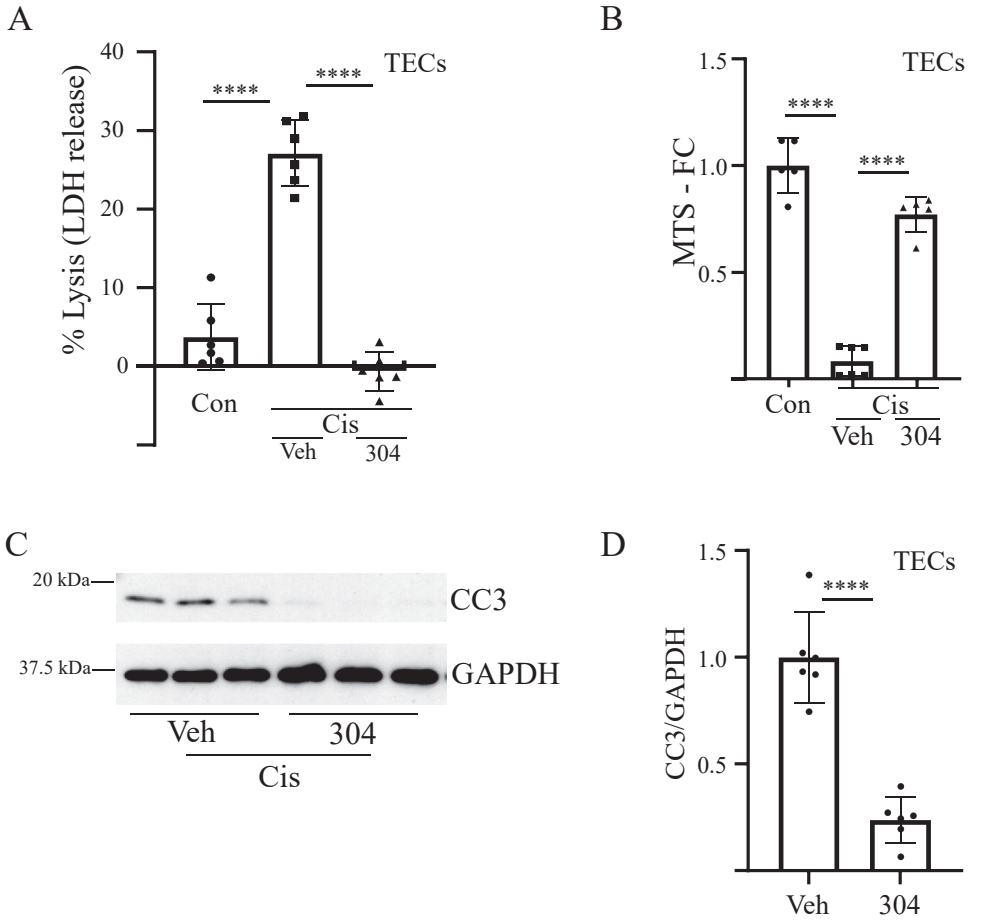

Fig. 4. ATX-304 protects TECs against cisplatin induced injury. TECs were pre-treated with ATX-304 20 μM for 4 h, ATX-304 was removed from the culture media, prior to exposing cells to cisplatin (cis) (20 μM for 23 h). A. Cellular injury measured by % lysis (LDH release). B. Cell viability measured by MTS assay measuring the formation of formazan by absorbance at 490 nm. C. Representative WB analysis of the effect of pre-treatment with ATX-304 compared with vehicle (Veh), on the expression of cleaved caspase 3 (CC3), normalized for GAPDH, after cisplatin exposure. D. Densitometry analysis of CC3 expression with ATX-304 prior to cisplatin. All data is shown as mean ± SD, **P <0.01, ***P <0.001, ****P <0.0001. Uncropped western blots supporting the data in this figure are available in the supplementary material.

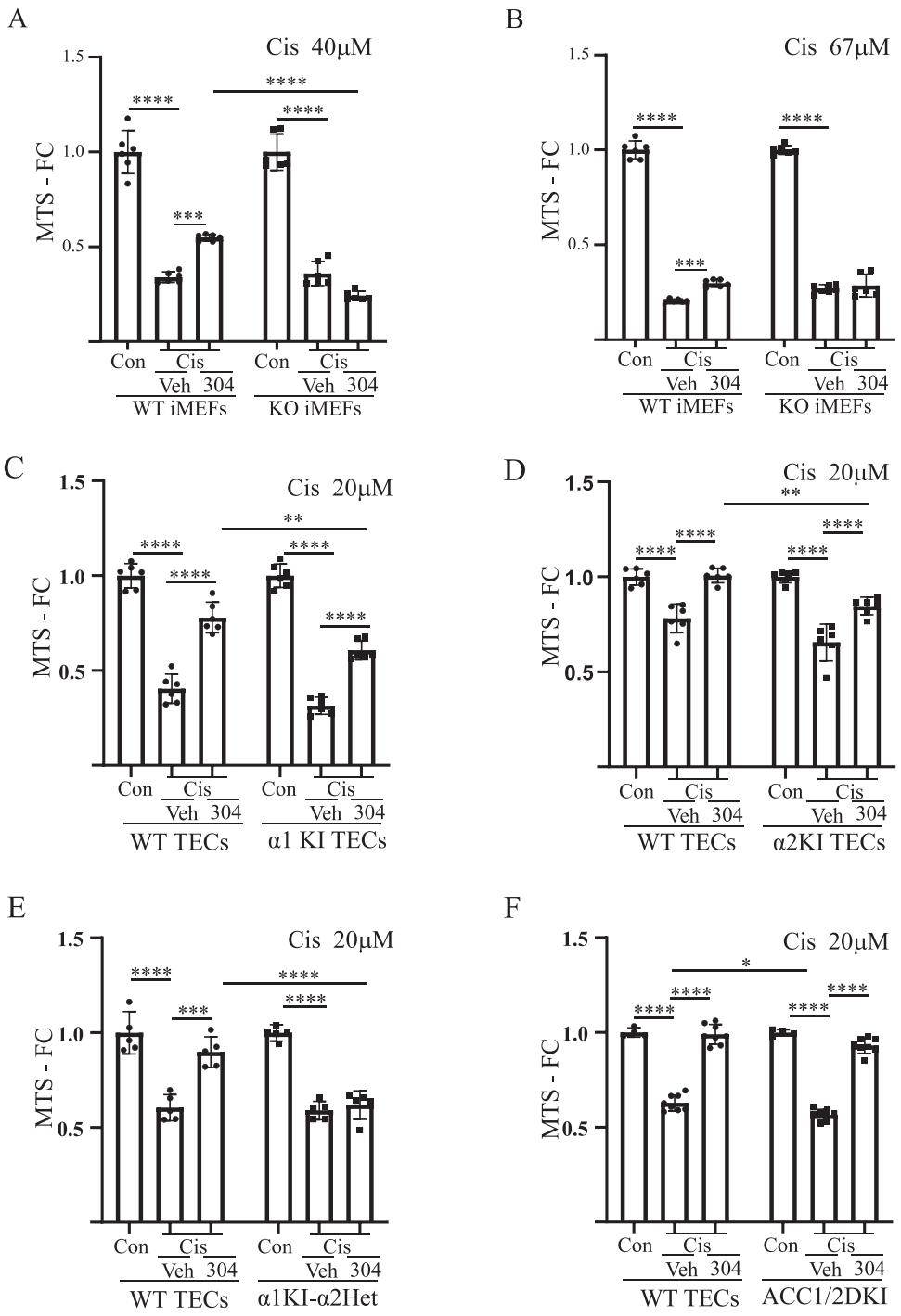

Fig. 5. ATX-304 protection against cisplatin-mediated injury is AMPK dependent. The effect of ATX-304 on cell viability in the setting of cisplatin was studied in WT and AMPK-β1/β2 KO iMEFs at 2 different cisplatin concentrations: (40 μM (5 A), 67 μM (5B)) for 23 h (n = 6 per group). *P <0.05, **P <0.01, ***P <0.001. MTS assay comparing the effect of ATX-304 on cell viability with cisplatin in WT and AMPK-α1 KI TECs (6 C). MTS assay comparing the effect of ATX-304 on cell viability with cisplatin in WT and AMPK-α2 KI TECs (5D). MTS assay of the effect of ATX-304 on cell viability with cisplatin in WT and αKI/α2Het TECs (5E). MTS assay comparing the effect of ATX-304 on cell viability with cisplatin in WT and ACC1/2DKI TECs (5 F). *P <0.05, **P <0.01, ***P <0.005, ****P <0.0001.

mutations. This crossbreeding generated some mice that were homozygous for α1KI and heterozygous for α2KI (α1KI/α2Het). In TECs from the α1KI/α2Het, MTS assay revealed that ATX-304 was not protective against cisplatin, consistent with the protective effect of ATX-304 against cisplatin being dependent on AMPK and involving contributions from both α1 and α2 heterotrimers of AMPK (Fig. 5E). To determine whether AMPK signaling to ACC is important for the protective effect of ATX-304 against cisplatin in TECs, TECs were isolated from ACC1/2 double knock-in (ACC1/2DKI) mice. A greater reduction in cell viability was observed with ACC1/2DKI TECs than with WT; however, ATX-304 remained protective in ACC1/2DKI TECs (Fig. 5F).

3.2.3. *Effect of ATX-304 on metabolite profile in tubular epithelial cells*

To better understand how ATX-304 protects kidney cells against injury, we examined the effect of ATX-304 (20 μM, 4 h) on TEC metabolism using metabolomic analysis (Fig. 6). Unsupervised principal component analysis demonstrated metabolome separation between ATX-304 treated and control TECs (Fig. 6A). Heatmap and dendrogram

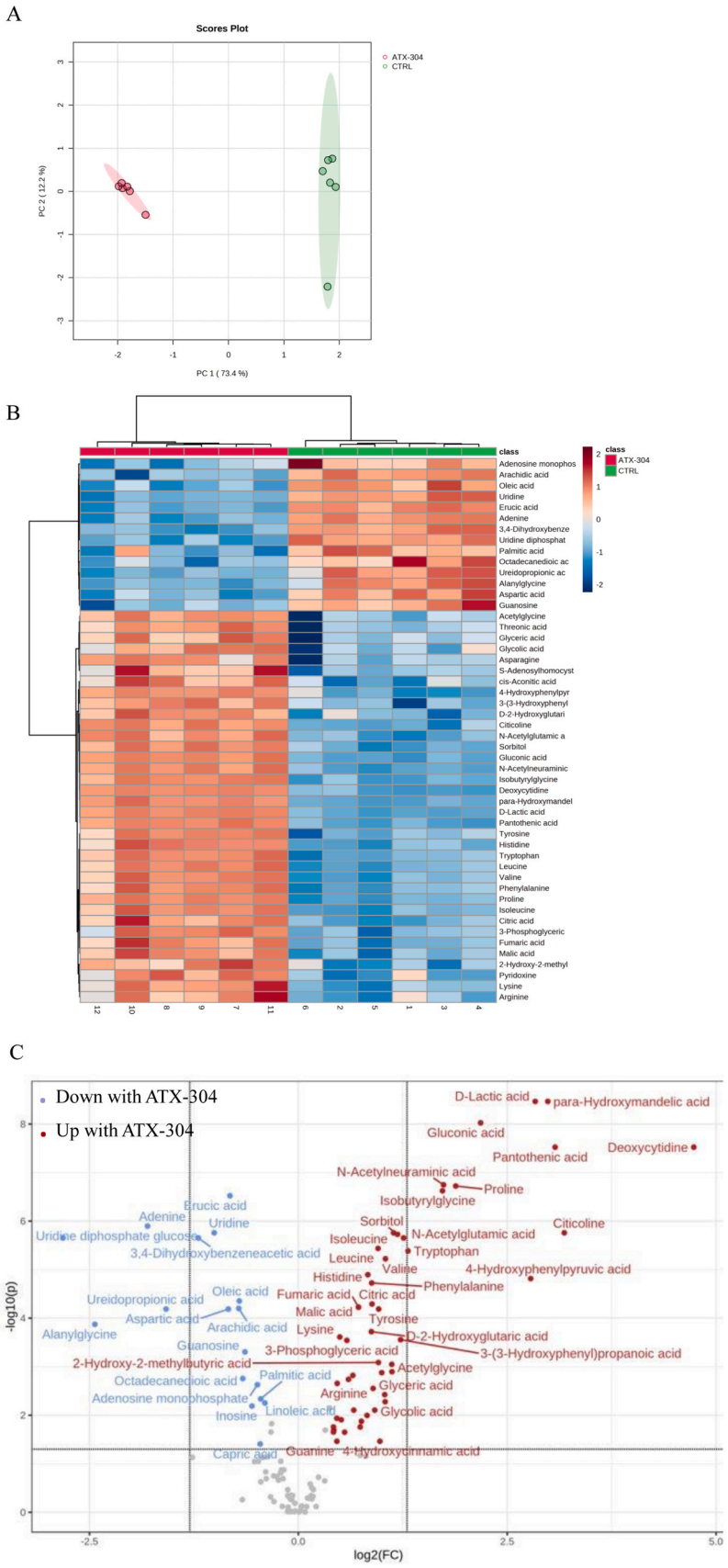

Fig. 6. ATX-304 treatment of TECs causes widespread alterations to the metabolome. A. Unsupervised principal component analysis comparing ATX-304 (20 μM, 4 h) versus control treated cells (n = 6 per group). The shaded areas represent the 95% confidence regions. B. Heatmap and dendogram analysis showing the 50 most different metabolites detected comparing ATX-304 with control treated TECs. C. Volcano plot analysis showing metabolites increased (red) or reduced (blue) with ATX-304. Thresholds for differences in this analysis were fold-change (FC) >1.3 and FDR P <0.05.

Table 1
Metabolite classes of interest affected by ATX-304 treatment of TECs. *P* values and FDRs were calculated in MetaboAnalyst using two-sample t-tests.

Metabolites	Fold-change ATX-304/control	*P*-value	FDR
Fatty Acids			
Erucic acid	0.57	2.15E-8	3.01E-7
Oleic acid	0.60	8.41E-6	4.42E-5
Arachidic acid	0.61	1.40E-5	6.30E-5
Palmitic acid	0.71	0.0018	0.005
Capric acid	0.73	0.002	0.039
Stearic acid	0.76	0.042	0.072
Linoleic acid	0.76	0.002	0.006
Citric acid cycle			
Citric acid	1.8	1.01E-5	5.11E-5
Fumaric acid	1.6	1.23E-5	5.94E-5
Malic acid	1.6	1.28E-5	5.95E-5
Cis-aconitic acid	1.5	5.05E-4	0.0015
Amino acids			
Proline	3.6	1.05E-8	1.89E-7
Tryptophan	2.4	6.23E-7	4.13E-6
Isoleucine	2.2	1.69E-7	1.74E-6
Valine	2.0	9.51E-7	5.99E-6
Leucine	1.9	5.22E-7	3.65E-6
Tyrosine	1.9	1.60E-5	6.50E-5
Phenylalanine	1.8	3.44E-6	1.88E-5
Histidine	1.7	2.12E-6	1.27E-5
Methionine	1.7	0.0045	0.010
Asparagine	1.5	6.37E-4	0.0018
Lysine	1.4	6.60E-5	2.44E-4
Arginine	1.3	7.90E-4	0.0022
Glycine	1.3	0.011	0.022
Threonine	1.3	0.010	0.020
Glutamine	0.96	0.94	0.96
Serine	0.93	0.34	0.45
Alanine	0.91	0.37	0.47
Cysteine	0.90	0.35	0.45
Glutamate	0.85	0.054	0.088
Aspartate	0.55	1.60E-5	6.50E-5
Glucose metabolism			
Lactic acid	7.01	4.89E-11	3.42E−9
Gluconic acid	4.46	2.25E-10	9.46E−9
Fructose	1.86	0.0034	0.0079
3-Phosphoglyceric acid	1.47	8.20E-5	2.87E−4
Glucose 6-phosphate	0.99	0.98	0.98
Fructose 6-phosphate	0.96	0.57	0.65
Glucose	0.87	0.68	0.75
6-Phosphogluconic acid	0.75	0.042	0.072
Nucleotides and nucleosides			
Uridine diphosphate glucose	0.14	1.80E-7	1.74E−6
Adenine	0.28	1.01E-7	1.27E−6
Uridine	0.49	1.80E-7	1.74E−6
Guanosine	0.63	1.46E-4	4.96E−4
Inosine	0.67	0.0027	0.0064
Adenosine monophosphate	0.70	8.57E-4	0.0023
Adenosine diphosphate	1.01	0.72	0.78
Guanine	1.36	0.019	0.034
Xanthine	1.65	0.038	0.067

analyses revealed clear partitioning of ATX-304 and control-treated TECs with differences across many metabolites (Fig. 6B). Volcano plot analysis identified 66/126 (52.4%) metabolites were altered by ATX-304 treatment, based on significance thresholds of fold-change (FC) > 1.3 and FDR $P < 0.05$ (Fig. 6C).

Analysis of metabolites of interest found that fatty acids were reduced by ATX-304, consistent with the expected effects of AMPK on fatty acid oxidation and synthesis[12], whereas citric acid cycle metabolites were increased (Table 1). In addition, ATX-304 treatment increased the levels of 14 amino acids. Analysis of the metabolites related to glucose metabolism revealed increased levels of lactate and 3-phosphoglycerate. No changes in glucose or glucose 6-phosphate were observed. Regarding nucleotides, as predicted with AMPK activation, ATX-304 reduced AMP levels, consistent with an overall reduction in energy stress. Various other nucleosides and nucleotides, such as uridine diphosphate, glucose, guanosine, and inosine, were also reduced in TECs

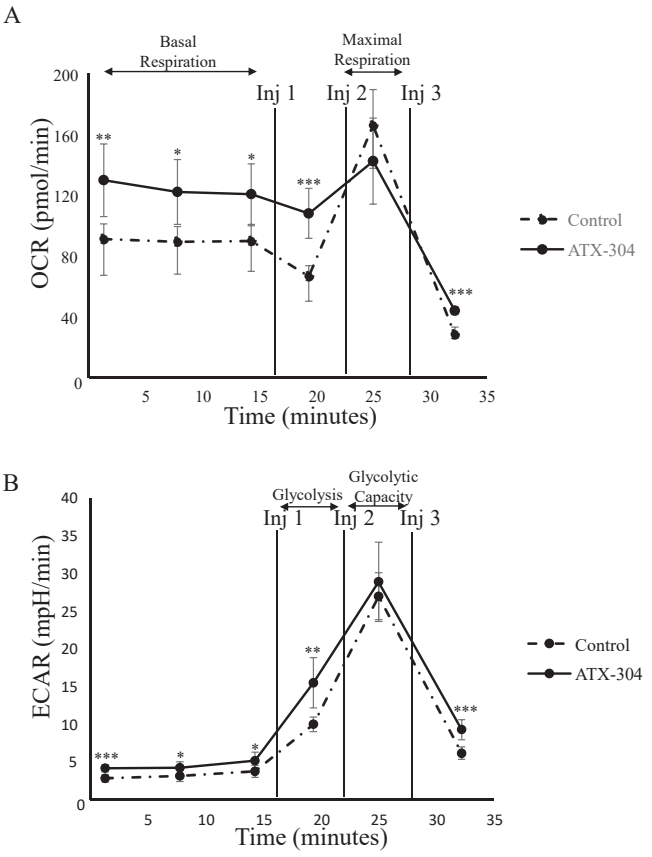

Fig. 7. ATX-304 causes changes in respiration and glycolysis in TECs. The XFe96 Seahorse analyzer was used to measure respiration in TECs as the oxygen consumption rate (OCR) (7 A) and glycolysis was measured as the extracellular acidification rate (ECAR) (7B). 40,000 TECs were analyzed per well. TECs were treated with ATX-304 (20 μM, 4 h) or control. For OCR analysis (7 A) the sequence of injections was injection 1 oligomycin, injection 2 FCCP, and injection 3 rotenone and antimycin A. For ECAR analysis (7B) the sequence of injections was injection 1 glucose, injection 2 oligomycin, injection 3 2-DG. *P <0.05, **P <0.01, ***P <0.005.

treated with ATX-304 (Table 1).

3.3. Effect of ATX-304 on TEC respiration and glycolysis

To further assess the effect of ATX-304 on energy metabolism in TECs, respiration and glycolysis were analyzed using the XFe96 Seahorse analyzer after ATX-304 treatment (20 μM, 4-h) compared to control (Fig. 7). After ATX-304 treatment, the basal oxygen consumption rate (OCR), a measure of mitochondrial oxidative phosphorylation, increased by 38% (Fig. 7A). The OCR remained elevated with ATX-304 treatment after oligomycin injection (injection 1), consistent with evidence of a proton leak. Maximal respiration was unchanged with ATX-304, indicating that ATX-304 diminished spare respiratory capacity (Fig. 7A). Regarding glycolysis, this was increased by 55% after ATX-304 treatment; however, the total glycolytic capacity was unchanged (Fig. 7B).

4. Discussion

In this investigation, the AMPK activator ATX-304 protected against cisplatin-mediated kidney injury, both in whole-animal CI-AKI and primary kidney TEC cultures. The findings in the present study of an increased basal oxygen consumption rate with ATX-304 in TECs, indicative of metabolic uncoupling, are consistent with a recent study describing a similar phenomenon in C2C12 myotubes [18].

Additionally, metabolomic analysis revealed that ATX-304 decreased AMP levels in TECs, implying an overall reduction in energy stress, in contrast to metformin, which is known to activate AMPK by increasing AMP [29,30]. Collectively, these data suggest that AMPK activation caused by ATX-304 may be attributable to a direct effect on αThr^{172} dephosphorylation, as well as an effect on mitochondrial uncoupling. The mechanism by which ATX-304 causes mitochondrial uncoupling has yet to be determined. In the present study, ATX-304 did not protect against cisplatin toxicity in AMPK-β1/β2 KO iMEFs, which, importantly, is the first direct genetic evidence demonstrating that a beneficial effect of ATX-304 is AMPK dependent. Furthermore, experiments on TECs from the AMPK-α1 and AMPK-α2 KI strains revealed that both α1 and α2 heterotrimers contributed to the protective action of ATX-304. Activation of AMPK by ATX-304 resulted in metabolic reprogramming of kidney TECs, as evidenced by the increased expression of metabolism genes, altered metabolite profiles, and altered metabolism in live cells. These findings underscore the potential of AMPK activation to protect against kidney injury by modulating energy metabolism.

AMPK, PCG1α, and sirtuins have been identified as important energy pathway targets for the treatment of kidney disease [28]. The present study is consistent with previous reports, showing that the renoprotective effect of AMPK activation involves the upregulation of PCG1α and sirtuins [28,31]. We observed that ATX-304 led to substantial increases in PCG1α and SIRT3 in TECs, both of which are known to enhance kidney protection via improved mitochondrial function [28,31]. This is consistent with an earlier study in CI-AKI, which found that activation of AMPK by 5-aminoimidazole-4-carboxamide-1-β-d-ribofuranoside (AICAR) maintained mitochondrial density and increased the expression of SIRT3 and PCG1α, and that this was protective against injury [31]. The effect of AMPK in increasing PCG1α involves both direct PGC1α phosphorylation [32] and indirect activation of PGC1α via sirtuins [33] and transcription factor EB [34]. SIRT1 has also been reported to be protective against CI-AKI [35], however, in our study SIRT-1 RNA expression was reduced with ATX-304, although a limitation in our study is that SIRT1 expression in the nucleus was not examined. Overall, these observations confirm that the effects of AMPK activation involve both rapid cytoplasmic effects on energy metabolism arising from protein phosphorylation events, and more sustained effects on energy metabolism arising from expression of genes important in metabolic and mitochondrial function.

Previous studies have found that metformin, a weak and indirect activator of AMPK, also protects against CI-AKI [14,36] as well as AKI from other causes such as sepsis [37] and ischemia [38]. The clinical utility of metformin for AKI is limited; however, by its association with lactic acidosis [39], caused by the inhibition of mitochondrial complex I [30]. An important advantage over metformin for novel AMPK activators such as ATX-304, could be the avoidance of lactic acidosis. However, further studies are required to assess this, and we observed in our metabolomic analysis that lactate levels were increased. Various natural compounds that activate AMPK, such as resveratrol [40], quercetin [41], and berberine [42], have also been reported to protect against AKI in experimental models. Mechanisms that have been identified as contributing to AMPK activation to protect against AKI include promoting autophagy [36], reducing inflammation and oxidative stress [43], improving mitochondrial function [31], and increasing fatty acid oxidation [14].

A useful feature of ATX-304, in contrast to earlier direct AMPK activators such as A-769662, is its effective oral bioavailability and activity [17]. The dose of ATX-304 used in the present study before CI-AKI induction was 1 mg/g in chow for seven days. This relatively low dose compares to a previous study using 2 mg/g in chow for 6 weeks, which was well tolerated and improved glucose metabolism in diet-induced obesity [17]. While the present study demonstrates ATX-304 protection against kidney injury, future studies are needed to determine the optimal dose and timing of therapy. The finding of protection against kidney injury in this study adds to the knowledge from previous studies that ATX-304 improves glucose homeostasis [17], metabolism, cardiac function, and exercise capacity [44]. The potential applicability of ATX-304 in human health is supported by a phase 2a clinical trial that found combining ATX-304 with metformin was well tolerated and improved glucose homeostasis and microvascular perfusion in patients with type 2 diabetes [17].

A strength of the present study is its unbiased documentation of the change in the metabolite profile that occurred with ATX-304 treatment of TECs, providing novel insights into the mechanisms of ATX-304 protection against injury. Fatty acids, including palmitic acid, oleic acid, and stearic acid, were reduced by ATX-304, consistent with the increase observed in ACC phosphorylation and the well-established effects of AMPK on fatty acid oxidation and synthesis [14]. Previously, we found that AMPK-mediated phosphorylation of ACC contributes to the protective effects of metformin [14,22]. In the present study, however, ATX-304 remained protective when AMPK signaling to ACC was blocked in ACC1/2DKI TECs, indicating that other effects of AMPK contribute to its protection. We also observed increased citric acid cycle metabolites, including citrate, fumarate, malate, and cis-aconitic acid, indicating increased activity of the mitochondrial tricarboxylic acid cycle, consistent with the observation of increased respiration in live cells with the Seahorse analyzer, as well as increased TEC expression of PGC1α and SIRT3 by RT-PCR. These data in the present study contrast to metabolomic profiling with metformin treatment in a previous study, which showed decreased metabolic flux from acetyl-CoA to the citric acid cycle [29]. Another observation of the present study was that ATX-304 increased the levels of multiple amino acids. This could signify AMPK activation reducing protein synthesis via its inhibitory effect on mTOR [13], or by AMPK activation increasing protein catabolism, a phenomenon associated with AMPK-induced autophagy through the phosphorylation of unc-51 like autophagy activating kinase 1 [45].

The significance of ATX-304 protective effects in the kidney may extend beyond mitigating cisplatin injury to other forms of acute and chronic kidney disease. For example, ATX-304 has also been reported to prevent aging-related kidney fibrosis [20]. Given that AMPK activation with various agents has been reported to be beneficial in kidney diseases associated with diabetes and obesity [46], evaluating the impact of ATX-304 in the kidney in the context of chronic metabolic conditions is of particular interest. Autosomal dominant polycystic kidney disease is another common cause of kidney failure and is increasingly recognized as an opportunity for the therapeutic application of AMPK activation [47], as illustrated by a recent report showing that the direct AMPK activator PXL770 ameliorates the progression of this disease [48].

In summary, our study demonstrates that the AMPK activator ATX-304 confers protection against cisplatin-mediated kidney injury in both an animal model and in primary kidney cells, with this effect being mediated by AMPK and associated with broad metabolic alterations. These findings underscore the potential of AMPK activation by ATX-304 as a novel therapeutic strategy for AKI and, potentially, other kidney diseases.

CRediT authorship contribution statement

David A Power: Writing – review & editing, Project administration, Methodology, Investigation, Funding acquisition, Formal analysis, Conceptualization. **Kim Loh:** Writing – review & editing, Resources, Methodology, Conceptualization. **Peter Mount:** Writing – review & editing, Writing – original draft, Validation, Supervision, Resources, Project administration, Methodology, Investigation, Funding acquisition, Formal analysis, Data curation, Conceptualization. **Jonathan Oakhill:** Writing – review & editing, Resources, Methodology, Formal analysis. **Bruce E Kemp:** Writing – review & editing, Resources, Conceptualization. **David P de Souza:** Writing – review & editing, Resources, Methodology, Investigation, Formal analysis. **Robert Brink:** Writing – review & editing, Resources, Methodology. **Mardiana Lee:** Writing – review & editing, Methodology, Formal analysis, Conceptualization. **Geoff Harley:** Writing – review & editing, Writing – original

draft, Methodology, Investigation, Formal analysis, Conceptualization. **Lisa Murray-Segal:** Writing – review & editing, Resources, Methodology. **Marina Katerelos:** Writing – review & editing, Writing – original draft, Project administration, Methodology, Investigation, Formal analysis, Data curation, Conceptualization. **Kurt Gleich:** Writing – review & editing, Methodology, Investigation. **Vinod Narayana:** Writing – review & editing, Resources, Methodology, Investigation, Formal analysis. **Melinda T Coughlan:** Writing – review & editing, Resources, Methodology, Investigation, Formal analysis. **Adrienne Laskowski:** Writing – review & editing, Methodology, Formal analysis. **Naomi X Y Ling:** Writing – review & editing, Resources, Methodology.

Declaration of Competing Interest

The authors declare the following financial interests/personal relationships which may be considered as potential competing interests: Amplifier Therapeutics (Betagenon) provided ATX-304 used in this study, however, Amplifier Therapeutics (Betagenon) did not contribute to the study design or contribute specific funding to the study. JSO has received payment from Amplifier Therapeutics (Betagenon) to perform mechanistic studies on ATX-304.

Data Availability

Data will be made available on request.

Acknowledgments

This study was funded by an Ideas Grant from the National Health and Medical Research Council (Government of Australia), Grant ID 2010600. ATX-304 was supplied by Amplifier Therapeutics (Cambrian Bio Pharma, Inc., NY, USA).

Appendix A. Supporting information

Supplementary data associated with this article can be found in the online version at doi:10.1016/j.biopha.2024.116730.

References

[1] C. Ronco, R. Bellomo, J.A. Kellum, Acute kidney injury, Lancet 394 (10212) (2019) 1949–1964.
[2] J.T. Kurzhagen, S. Dellepiane, V. Cantaluppi, H. Rabb, AKI: an increasingly recognized risk factor for CKD development and progression, J. Nephrol. 33 (6) (2020) 1171–1187.
[3] A.J. Clark, S.M. Parikh, Mitochondrial metabolism in acute kidney injury, Semin Nephrol. 40 (2) (2020) 101–113.
[4] D.P. Basile, M.D. Anderson, T.A. Sutton, Pathophysiology of acute kidney injury, Compr. Physiol. 2(2 (2012) 1303–1353.
[5] Z.Y. Bhat, P. Cadnapaphornchai, K. Ginsburg, M. Sivagnanam, S. Chopra, C. K. Treadway, H.S. Lin, G. Yoo, A. Sukari, M.D. Doshi, Understanding the risk factors and long-term consequences of cisplatin-associated acute kidney injury: an observational cohort study, PLoS One 10 (11) (2015) e0142225.
[6] S. Negi, D. Koreeda, S. Kobayashi, T. Yano, K. Tatsuta, T. Mima, T. Shigematsu, M. Ohya, Acute kidney injury: epidemiology, outcomes, complications, and therapeutic strategies, Semin Dial. 31 (5) (2018) 519–527.
[7] H.S. Jang, M.R. Noh, J. Kim, B.J. Padanilam, Defective mitochondrial fatty acid oxidation and lipotoxicity in kidney diseases, Front Med 7 (2020) 65.
[8] H.M. Kang, S.H. Ahn, P. Choi, Y.A. Ko, S.H. Han, F. Chinga, A.S. Park, J. Tao, K. Sharma, J. Pullman, E.P. Bottinger, I.J. Goldberg, K. Susztak, Defective fatty acid oxidation in renal tubular epithelial cells has a key role in kidney fibrosis development, Nat. Med 21 (1) (2015) 37–46.
[9] R. Rajani, N.M. Pastor-Soler, K.R. Hallows, Role of AMP-activated protein kinase in kidney tubular transport, metabolism, and disease, Curr. Opin. Nephrol. Hypertens. 26 (5) (2017) 375–383.
[10] G.R. Steinberg, D.G. Hardie, New insights into activation and function of the AMPK, Nat. Rev. Mol. Cell Biol. 24 (4) (2023) 255–272.
[11] S. Herzig, R.J. Shaw, AMPK: guardian of metabolism and mitochondrial homeostasis, Nat. Rev. Mol. Cell Biol. 19 (2) (2018) 121–135.
[12] Y. Li, Y. Chen, AMPK and autophagy, Adv. Exp. Med Biol. 1206 (2019) 85–108.
[13] Y. Wang, Z. Liu, S. Shu, J. Cai, C. Tang, Z. Dong, AMPK/mTOR Signaling in Autophagy Regulation During Cisplatin-Induced Acute Kidney Injury, Front Physiol. 11 (2020) 619730.
[14] G. Harley, M. Katerelos, K. Gleich, D.P. de Souza, V.K. Narayana, B.E. Kemp, D. A. Power, P.F. Mount, Blocking AMPK signalling to acetyl-CoA carboxylase increases cisplatin-induced acute kidney injury and suppresses the benefit of metformin, Biomed. Pharm. 153 (2022) 113377.
[15] H. Ma, X. Guo, S. Cui, Y. Wu, Y. Zhang, X. Shen, C. Xie, J. Li, Dephosphorylation of AMP-activated protein kinase exacerbates ischemia/reperfusion-induced acute kidney injury via mitochondrial dysfunction, Kidney Int 101 (2) (2022) 315–330.
[16] C. Tan, J. Gu, T. Li, H. Chen, K. Liu, M. Liu, H. Zhang, X. Xiao, Inhibition of aerobic glycolysis alleviates sepsis-induced acute kidney injury by promoting lactate/Sirtuin 3/AMPK-regulated autophagy, Int J. Mol. Med 47 (3) (2021).
[17] P. Steneberg, E. Lindahl, U. Dahl, E. Lidh, J. Straseviciene, F. Backlund, E. Kjellkvist, E. Berggren, I. Lundberg, I. Bergqvist, M. Ericsson, B. Eriksson, K. Linde, J. Westman, T. Edlund, H. Edlund, PAN-AMPK activator O304 improves glucose homeostasis and microvascular perfusion in mice and type 2 diabetes patients, JCI Insight 3 (12) (2018).
[18] S. Norlin, J. Axelsson, M. Ericsson, H. Edlund, O304 ameliorates hyperglycemia in mice by dually promoting muscle glucose effectiveness and preserving beta-cell function, Commun. Biol. 6 (1) (2023) 877.
[19] R.W. Myers, H.P. Guan, J. Ehrhart, A. Petrov, S. Prahalada, E. Tozzo, X. Yang, M. M. Kurtz, M. Trujillo, D. Gonzalez Trotter, D. Feng, S. Xu, G. Eiermann, M. A. Holahan, D. Rubins, S. Conarello, X. Niu, S.C. Souza, C. Miller, J. Liu, K. Lu, W. Feng, Y. Li, R.E. Painter, J.A. Milligan, H. He, F. Liu, A. Ogawa, D. Wisniewski, R.J. Rohm, L. Wang, M. Bunzel, Y. Qian, W. Zhu, H. Wang, B. Bennet, L. LaFranco Scheuch, G.E. Fernandez, C. Li, M. Klimas, G. Zhou, M. van Heek, T. Biftu, A. Weber, D.E. Kelley, N. Thornberry, M.D. Erion, D.M. Kemp, I.K. Sebhat, Systemic pan-AMPK activator MK-8722 improves glucose homeostasis but induces cardiac hypertrophy, Science 357 (6350) (2017) 507–511.
[20] M. Zhu, W. Shen, J. Li, N. Jia, Y. Xiong, J. Miao, C. Xie, Q. Chen, K. Shen, P. Meng, X. Li, Q. Wu, S. Zhou, M. Wang, Y. Kong, L. Zhou, AMPK Activator O304 Protects Against Kidney Aging Through Promoting Energy Metabolism and Autophagy, Front Pharm. 13 (2022) 836496.
[21] C. Kilkenny, W.J. Browne, I.C. Cuthill, M. Emerson, D.G. Altman, Improving bioscience research reporting: the ARRIVE guidelines for reporting animal research, PLoS Biol. 8 (6) (2010) e1000412.
[22] M. Lee, M. Katerelos, K. Gleich, S. Galic, B.E. Kemp, P.F. Mount, D.A. Power, Phosphorylation of Acetyl-CoA carboxylase by AMPK reduces renal fibrosis and is essential for the anti-fibrotic effect of metformin, J. Am. Soc. Nephrol. 29 (9) (2018) 2326–2336.
[23] T.A. Dite, N.X.Y. Ling, J.W. Scott, A. Hoque, S. Galic, B.L. Parker, K.R.W. Ngoei, C. G. Langendorf, M.T. O'Brien, M. Kundu, B. Viollet, G.R. Steinberg, K. Sakamoto, B. E. Kemp, J.S. Oakhill, The autophagy initiator ULK1 sensitizes AMPK to allosteric drugs, Nat. Commun. 8 (1) (2017) 571.
[24] H. Yang, H. Wang, R. Jaenisch, Generating genetically modified mice using CRISPR/Cas-mediated genome engineering, Nat. Protoc. 9 (8) (2014) 1956–1968.
[25] P.F. Mount, K. Gleich, S. Tam, S.A. Fraser, S.W. Choy, K.M. Dwyer, B. Lu, B. V. Denderen, G. Fingerle-Rowson, R. Bucala, B.E. Kemp, D.A. Power, The outcome of renal ischemia-reperfusion injury is unchanged in AMPK-beta1 deficient mice, PLoS One 7 (1) (2012) e29887.
[26] R.J. Stewart, L. Whitehead, B. Nijagal, B.E. Sleebs, G. Lessene, M.J. McConville, K. L. Rogers, C.J. Tonkin, Analysis of Ca(2)(+) mediated signaling regulating Toxoplasma infectivity reveals complex relationships between key molecules, Cell Microbiol 19 (4) (2017).
[27] L.W. Sumner, A. Amberg, D. Barrett, M.H. Beale, R. Beger, C.A. Daykin, T.W. Fan, O. Fiehn, R. Goodacre, J.L. Griffin, T. Hankemeier, N. Hardy, J. Harnly, R. Higashi, J. Kopka, A.N. Lane, J.C. Lindon, P. Marriott, A.W. Nicholls, M.D. Reily, J. J. Thaden, M.R. Viant, Proposed minimum reporting standards for chemical analysis Chemical Analysis Working Group (CAWG) Metabolomics Standards Initiative (MSI), Metabolomics 3 (3) (2007) 211–221.
[28] A.J. Clark, S.M. Parikh, Targeting energy pathways in kidney disease: the roles of sirtuins, AMPK, and PGC1alpha, Kidney Int 99 (4) (2021) 828–840.
[29] M. Yan, H. Qi, T. Xia, X. Zhao, W. Wang, Z. Wang, C. Lu, Z. Ning, H. Chen, T. Li, D. S. Tekcham, X. Liu, J. Liu, D. Chen, X. Liu, G. Xu, H.L. Piao, Metabolomics profiling of metformin-mediated metabolic reprogramming bypassing AMPKalpha, Metabolism 91 (2019) 18–29.
[30] G. Rena, D.G. Hardie, E.R. Pearson, The mechanisms of action of metformin, Diabetologia 60 (9) (2017) 1577–1585.
[31] M. Morigi, L. Perico, C. Rota, L. Longaretti, S. Conti, D. Rottoli, R. Novelli, G. Remuzzi, A. Benigni, Sirtuin 3-dependent mitochondrial dynamic improvements protect against acute kidney injury, J. Clin. Invest 125 (2) (2015) 715–726.
[32] S. Jager, C. Handschin, J. St-Pierre, B.M. Spiegelman, AMP-activated protein kinase (AMPK) action in skeletal muscle via direct phosphorylation of PGC-1alpha, Proc. Natl. Acad. Sci. USA 104 (29) (2007) 12017–12022.
[33] C. Canto, Z. Gerhart-Hines, J.N. Feige, M. Lagouge, L. Noriega, J.C. Milne, P. J. Elliott, P. Puigserver, J. Auwerx, AMPK regulates energy expenditure by modulating NAD+ metabolism and SIRT1 activity, Nature 458 (7241) (2009) 1056–1060.
[34] Y. Nakamura, Y. Yanagawa, S.F. Morrison, K. Nakamura, Medullary Reticular Neurons Mediate Neuropeptide Y-Induced Metabolic Inhibition and Mastication, Cell Metab. 25 (2) (2017) 322–334.
[35] K. Hasegawa, S. Wakino, K. Yoshioka, S. Tatematsu, Y. Hara, H. Minakuchi, K. Sueyasu, N. Washida, H. Tokuyama, M. Tzukerman, K. Skorecki, K. Hayashi, H. Itoh, Kidney-specific overexpression of Sirt1 protects against acute kidney injury by retaining peroxisome function, J. Biol. Chem. 285 (17) (2010) 13045–13056.
[36] J. Li, Y. Gui, J. Ren, X. Liu, Y. Feng, Z. Zeng, W. He, J. Yang, C. Dai, Metformin Protects Against Cisplatin-Induced Tubular Cell Apoptosis and Acute Kidney Injury via AMPKalpha-regulated Autophagy Induction, Sci. Rep. 6 (2016) 23975.

[37] K. Jin, Y. Ma, C.L. Manrique-Caballero, H. Li, D.R. Emlet, S. Li, C.J. Baty, X. Wen, N. Kim-Campbell, A. Frank, E.V. Menchikova, N.M. Pastor-Soler, K.R. Hallows, E. K. Jackson, S. Shiva, M.R. Pinsky, B.S. Zuckerbraun, J.A. Kellum, H. Gomez, Activation of AMP-activated protein kinase during sepsis/inflammation improves survival by preserving cellular metabolic fitness, FASEB J. 34 (5) (2020) 7036–7057.
[38] P.W. Seo-Mayer, G. Thulin, L. Zhang, D.S. Alves, T. Ardito, M. Kashgarian, M. J. Caplan, Preactivation of AMPK by metformin may ameliorate the epithelial cell damage caused by renal ischemia, Am. J. Physiol. Ren. Physiol. 301 (6) (2011) F1346–F1357.
[39] R. DeFronzo, G.A. Fleming, K. Chen, T.A. Bicsak, Metformin-associated lactic acidosis: Current perspectives on causes and risk, Metabolism 65 (2) (2016) 20–29.
[40] S. Cao, X. Fu, S. Yang, S. Tang, The anti-inflammatory activity of resveratrol in acute kidney injury: a systematic review and meta-analysis of animal studies, Pharm. Biol. 60 (1) (2022) 2088–2097.
[41] Y. Wang, F. Quan, Q. Cao, Y. Lin, C. Yue, R. Bi, X. Cui, H. Yang, Y. Yang, L. Birnbaumer, X. Li, X. Gao, Quercetin alleviates acute kidney injury by inhibiting ferroptosis, J. Adv. Res 28 (2021) 231–243.
[42] M. Adil, A.D. Kandhare, G. Dalvi, P. Ghosh, S. Venkata, K.S. Raygude, S. L. Bodhankar, Ameliorative effect of berberine against gentamicin-induced nephrotoxicity in rats via attenuation of oxidative stress, inflammation, apoptosis and mitochondrial dysfunction, Ren. Fail 38 (6) (2016) 996–1006.
[43] L. Gong, Q. Pan, N. Yang, Autophagy and inflammation regulation in acute kidney injury, Front Physiol. 11 (2020) 576463.
[44] M. Ericsson, P. Steneberg, R. Nyren, H. Edlund, AMPK activator O304 improves metabolic and cardiac function, and exercise capacity in aged mice, Commun. Biol. 4 (1) (2021) 1306.
[45] S. Wang, H. Li, M. Yuan, H. Fan, Z. Cai, Role of AMPK in autophagy, Front Physiol. 13 (2022) 1015500.
[46] F. Juszczak, N. Caron, A.V. Mathew, A.E. Decleves, Critical Role for AMPK in Metabolic Disease-Induced Chronic Kidney Disease, Int J. Mol. Sci. 21 (21) (2020).
[47] I.A. Iliuta, X. Song, L. Pickel, A. Haghighi, R. Retnakaran, J. Scholey, H.K. Sung, G. R. Steinberg, Y. Pei, Shared pathobiology identifies AMPK as a therapeutic target for obesity and autosomal dominant polycystic kidney disease, Front Mol. Biosci. 9 (2022) 962933.
[48] P.G. Dagorn, B. Buchholz, A. Kraus, B. Batchuluun, H. Bange, L. Blockken, G. R. Steinberg, D.E. Moller, S. Hallakou-Bozec, A novel direct adenosine monophosphate kinase activator ameliorates disease progression in preclinical models of Autosomal Dominant Polycystic Kidney Disease, Kidney Int 103 (5) (2023) 917–929.